Fermi National Accelerator Laboratory

FERMILAB-TM-1899

The Effect of Azimuthal Inert Material on the CMS Hadron Calorimeter

Dan Green

Fermi National Accelerator Laboratory
P.O. Box 500, Batavia, Illinois 60510

August 1994

Operated by Universities Research Association Inc. under Contract No. DE-AC02-76CHO3000 with the United States Department of Energy

Disclaimer

The Effect of Azimuthal Inert Material on the CMS Hadron Calorimeter

Dan Green
Fermilab
August 4, 1994

Introduction:

The baseline design for the CMS hadronic calorimeter (HCAL) calls for barrel wedges subtending an azimuthal range of 1/18 of 2 π. These wedges will each have about 1 cm of inert material which is required to make a self supporting structure. Therefore, it is expected that there will be about 2 cm of inert material between active elements in the CMS calorimeter. Since the inner radius of the HCAL modules is at 1.95 m, there is about 3% of the azimuth which is inert and *possibly* projective.

Previous studies for the SDC endcap have indicated that such a level of inert material is largely benign [1]. However, it is necessary to examine the specific case of CMS, both in the barrel and in the endcap.

The Model; Transverse and Longitudinal Cascades:

The model which was used assumed a parametrized transverse cascade development based on data taken with a steel calorimeter [2]. The data was embellished by assuming that the transverse size parameters increased linearly with the depth of the shower, as observed in other experiments [3].

Monte Carlo output for the transverse shower development is shown in Fig.1. The rms of a one dimensional transverse projection is shown in Fig1.a to increase linearly with depth of the cascade. At 80 cm (~ 4.8 λ) the rms is 15 cm of steel. The radial shower distribution at depths of 40 and 80 cm are given in Fig.1b. The model of ref. 1 was used which has two components, a central core, and a long tail. Both components are assumed to increase in size linearly with depth.

Hadronic showers are rather difficult to model well, as the intrinsic fluctuations are large. To avoid this issue, test beam data taken with hadrons incident on a neutrino detector were used [4]. Data at 50, 100, 200, and 450 GeV were used as a "shower library". Events were picked at random out of this library. The CMS barrel was modelled using this very deep steel calorimeter data. The EM was taken to be 1.0 λ deep, followed by HAD1 to a depth of 3.1 λ. The HAD2 compartment then continued the calorimeter coverage to 5.9 λ. Energy deposited deeper than that was defined to be leakage energy. In all that follows the resulting energy is normalized to the measured energy in the very deep neutrino calorimeter. Thus the quoted errors are due only to the dead

material. The effects of resolution and limited depth are not added to the basic measurement error due to inert material which is thus isolated for study.

The distribution of energy deposits in the various calorimeter compartments for 450 GeV incident hadrons is shown in Fig.2. The mean energies and percentages of the total energy are; <EEM> = 63.6 GeV (14.1%), <EHAD1> = 191.2 GeV (42.5%), <EHAD2> = 139.4 GeV (31%), and leakage <EL> = 56.2 GeV (12.5%). Clearly, HAD1 and HAD2 measure the bulk of the energy, and inert material within these two compartments potentially could increase energy measurement errors substantially.

Single Particle Response; Doglegs:

The effect of the magnetic field has been ignored in the present model. It seems intuitively obvious that the 4 T field in CMS will spread the showers, and therefore alleviate the effect of inert material. Therefore, the field free case has been pursued since it was thought to be a worst case scenario.

Several parameters are available for optimization. Most importantly, a scale for the allowable width of the dead material should be set. For that reason thicknesses of 2 and 4 cm were studied. A comparison of a projective 2 cm inert region was made to that of a "dogleg" where the centerline of inert material is offset between the HAD1 and HAD2 compartments. The former structure is easiest to manufacture, but the latter is expected to have less severe effects due to the inert material. The offset was always taken to be twice the thickness of the dead material, xd. Thus, HAD1 possessed dead material in the region (0, xd) while HAD2 had inert material from (2xd, 3xd) in the dogleg case, or (0, xd) in the projective case.

The results for the mean and rms of the energy distribution for a 2 cm wide dogleg are shown in Fig.3 as a function of the value of the incident transverse impact point x. The mean is shifted by up to 12%. The width of the region over which the shift in the mean is > 5% is about 10 cm or about 15% of the total azimuth. In principle the mean can be corrected for, but the rms cannot. The rms error caused by the inert material alone is about 5%, and exceeds 2% for about 10 cm or 15% of the total azimuth.

The results for a 4 cm inert width are shown in Fig.4. In this case the shift in the mean is up to 21% and exceeds 5% for 18 cm. Therefore, the damage to the resolution is roughly linear in the width of the inert material. The rms due to the inert material is up to 7.5% and exceeds 2% for about 23 cm. Note also the characteristic asymmetric behavior of both the mean and the rms as the incident "beam" is swept over the HAD1 and HAD2 doglegs. Clearly, the width of the effect is increased by using a dogleg structure.

The response to a projective structure with inert material is shown in Fig.5. In comparison to Fig.3, the shift in the mean is symmetric about x=1 cm, larger than the dogleg case, but spread over a smaller x range than the dogleg case. The maximum shift in the mean is 16% (compare to 12%). The region over which the shift in the mean exceeds 5% is about 8 cm (compare to 10

cm). The rms rises to 5.3% (compare to 5.2%) and exceeds 2% for about 10 cm (compare to 10 cm). Comparing Fig.5 to Fig.3 it is clear that the dogleg structure offers better response and should be chosen if other factors do not arise to disfavor this type of structure.

Higher moments of the energy distribution do not appear to be adversely effected. Fig.6 shows the energy distribution for a 2 cm thick inert region, with a dogleg structure, and with a single particle incident on the centerline of the HAD1 inert material (worst case). Clearly, there is a 12% shift in the mean and roughly 5% rms induced by the existence of the dead material. However, there is not a severe tail which would lead to a spurious missing Et signal. At the 1% level the worst mismeasurement is 67 GeV, or 24% of the mean.

Jet Response:

The CMS HCAL has the task of measuring neutrinos (missing Et) and jets due to hadronization of quarks and gluons. Therefore, the true Physics entity for CMS is the jet, not a single hadron. To that end, jets were modelled as ensembles of pions, charged and neutral. A neutral pion was assumed to deposit all its energy in the ECAL and the ECAL was assumed to possess no inert material. The pion fragmentation function was chosen to be:

$$zD(z) = (1-z)^5 \tag{1}$$

A jet of 2 TeV was chosen as that energy is close to the maximum observable jet Et at the LHC. The longitudinal response for charged hadrons was picked out of the energy nearest to the pion energy in the shower library. The transverse response was modelled using the single particle transverse model, assumed to be energy independent.

The energies deposited in the various CMS calorimeter compartments is shown in Fig.7 which is the 2 TeV jet analog of the 450 GeV single particle plots shown in Fig.2. The mean values are for EM 49%, for HAD1 25%, for HAD2 18%, and 8% leakage. Note that the leading pion has <z> ~ 0.2 or 400 GeV for the 2 TeV jet. Thus except for the neutral energy in the jet which enhances the EM fraction, the HAD and leakage fractions for Fig.7 and Fig.2 are roughly similar.

The jet energy observed for the jet axis incident on the center line of the HAD1 inert material (2 cm wide) is shown in Fig.8. This is thought to be the worst case. The shift in the mean jet energy is 7% and the induced rms is 2.8%. Note that the CMS magnetic field will make the mean shift and the induced rms more benign. Note also that these worst case results are less than what is intrinsic to a jet due to the definition of a jet, and the effects of pileup [5].

Therefore, the conclusion is that for CMS HCAL structures with up to 2 cm of azimuthal dead material will not compromise the purposes of HCAL. A dogleg structure alleviates some of the effects of this dead material. The effects due to magnetic field have not yet been evaluated, but are thought to soften the effects of the dead material.

References:

1. D. Green, Fermilab TM-1810 (1992).

2. A. L. Sessons et al., Nuc. Inst. and Meth. 161 371 (1979) and
   V. A. Davidov et al., Nuc. Inst. and Meth. 174 369 (1980).

3. S. Iwata, DPNU-3-79, Feb. 1979.

4. A. Beretvas - private communication.

5. D. Green, Fermilab Conf.-90/151 (1990).

Figure Captions:

Figure 1.a. The rms of the transverse distribution of hadronic energy deposited in a cascade as a function of the depth of the shower in cm of Fe.

1.b. The radial (transverse) distribution of hadronic energy deposited in a cascade in cm of Fe at a depth of 40 cm of Fe, 0, and 80 cm of Fe, *.

Figure 2. Energy deposited in various longitudinal compartments for 450 GeV hadrons incident on the CMS barrel calorimeter.
a. energy deposited in EM
b. energy deposited in HAD1
c. energy deposited in HAD2
d. energy deposited in material deeper than HAD2

Figure 3. Energy response for 100 GeV single hadrons incident on a structure with 2 cm dead material and a 4 cm offset between the dead material in HAD1 and that in HAD2.
a. energy mean as a function of incident position
b. energy rms as a function of incident position

Figure 4. Energy response for 100 GeV single hadrons incident on a structure with 4 cm dead material and a 8 cm offset between the dead material in HAD1 and that in HAD2.
a. energy mean as a function of incident position
b. energy rms as a function of incident position

Figure 5. Energy response for 100 GeV incident hadrons incident on a structure with 2 cm dead material and with no offset between the dead material in HAD1 and that in HAD2.
a. energy mean as a function of incident position
b. energy rms as a function of incident position

Figure 6. Energy distribution for 100 GeV hadrons incident on a structure with 2 cm dead material and with a 2 cm offset between the dead material in HAD1 and that in HAD2. The hadrons are incident on the center line of the HAD1 dead material, x=1 cm.

Figure 7. Energy deposited in various longitudinal compartments for a 2 TeV jet incident on the CMS barrel calorimeter.
a. energy deposited in EM
b. energy deposited in HAD1
c. energy deposited in HAD2
d. energy deposited in material deeper than HAD2

Figure 8. Energy distribution for 2 TeV jets incident on a structure with 2 cm dead material and with a 2 cm offset between the dead material in HAD1 and that in HAD2. The jet axis is incident on the center line of the HAD1 dead material, x=1 cm.

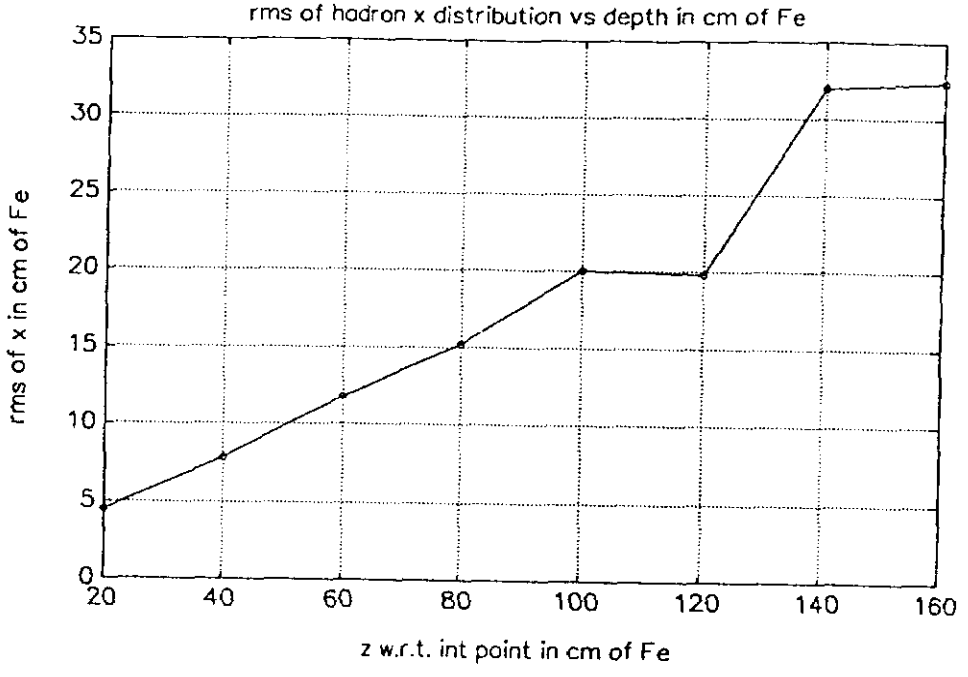

a)

Fig.. 1.a.

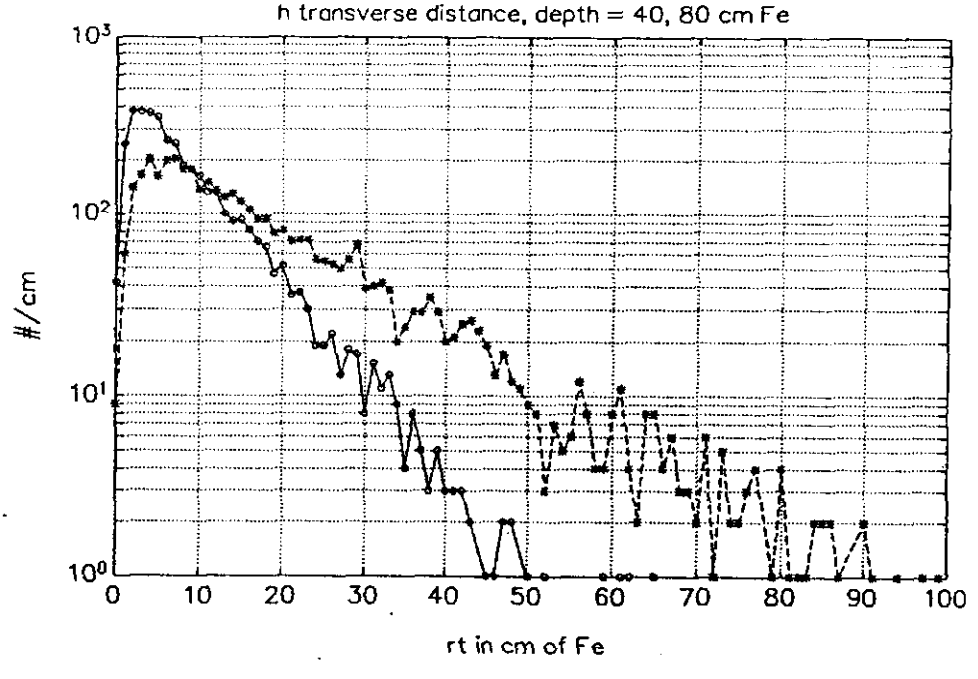

b)

Fig. 1.b.

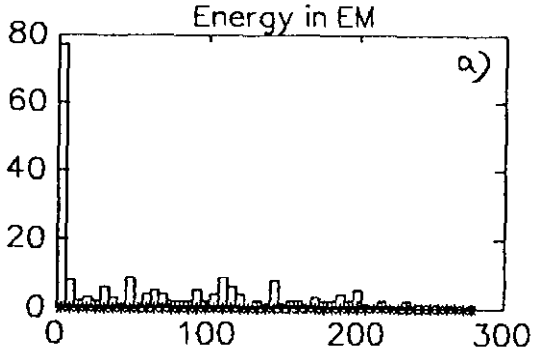

Fig. 2.a.

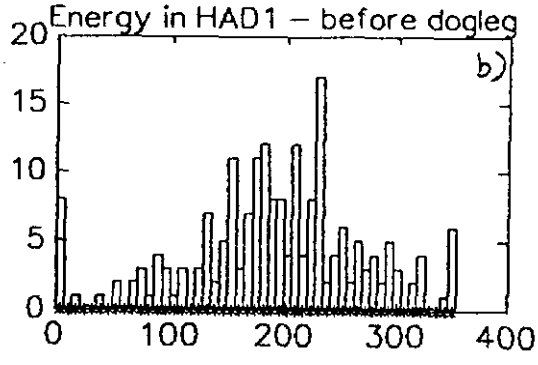

Fig. 2.b.

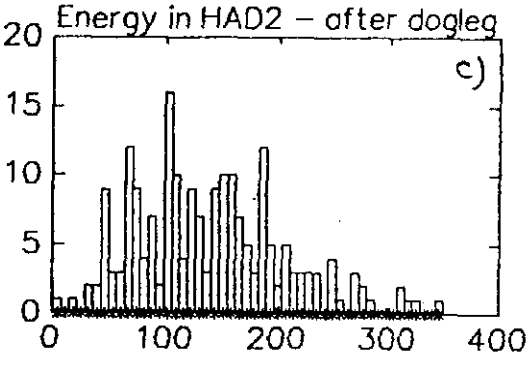

Fig. 2.c.

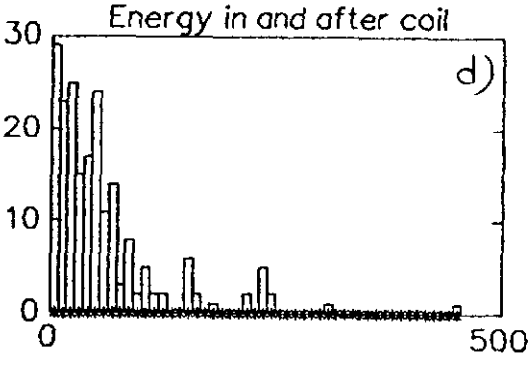

Fig. 2.d.

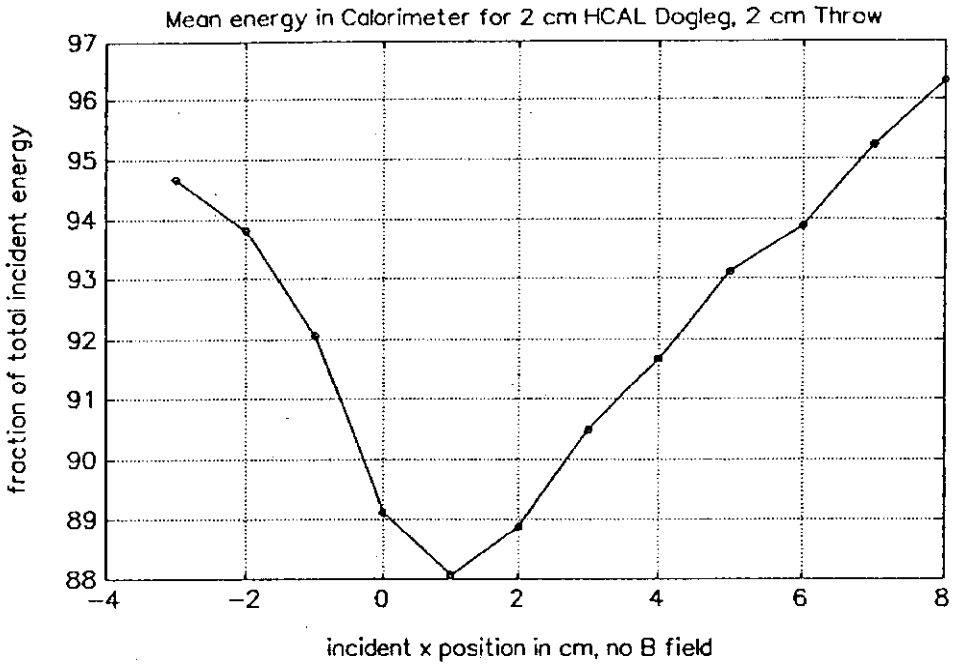

a)

Fig. 3.a.

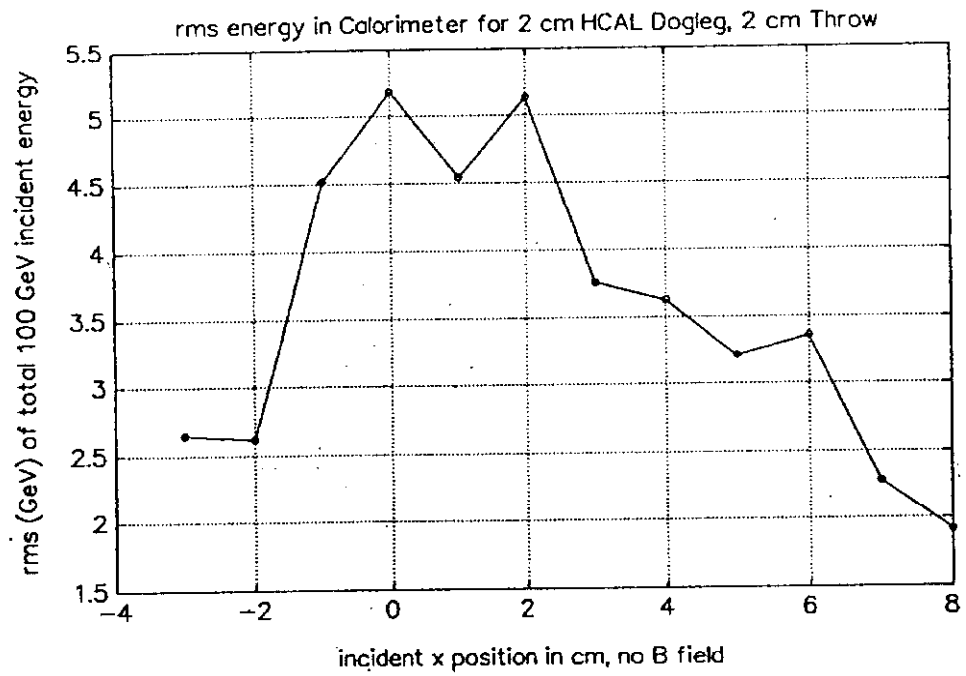

b)

Fig. 3.b.

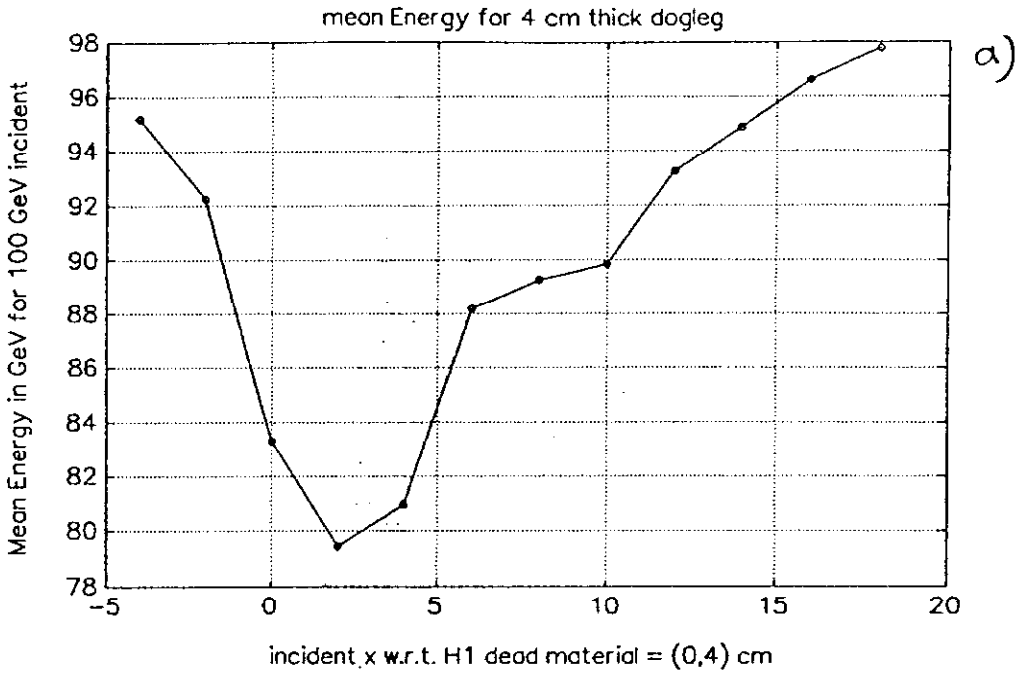
meon Energy for 4 cm thick dogleg
a)
Mean Energy in GeV for 100 GeV incident
98
96
94
92
90
88
86
84
82
80
78
-5
0
5
10
15
20
incident x w.r.t. H1 dead material = (0,4) cm

Fig. 4.a.

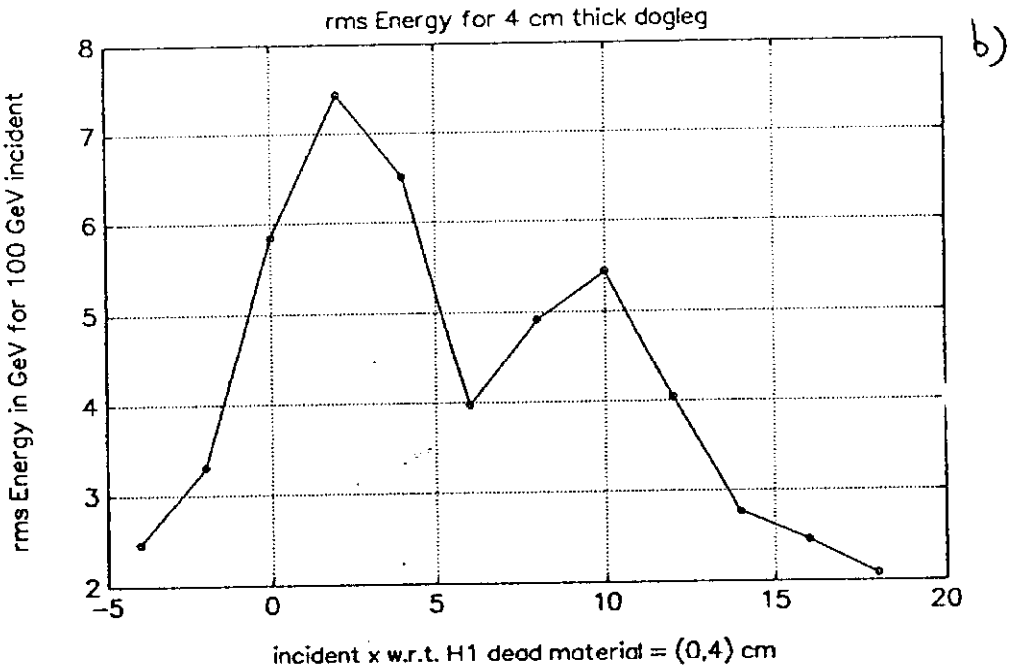
rms Energy for 4 cm thick dogleg
b)
rms Energy in GeV for 100 GeV incident
8
7
6
5
4
3
2
-5
0
5
10
15
20
incident x w.r.t. H1 dead material = (0,4) cm

Fig. 4.b.

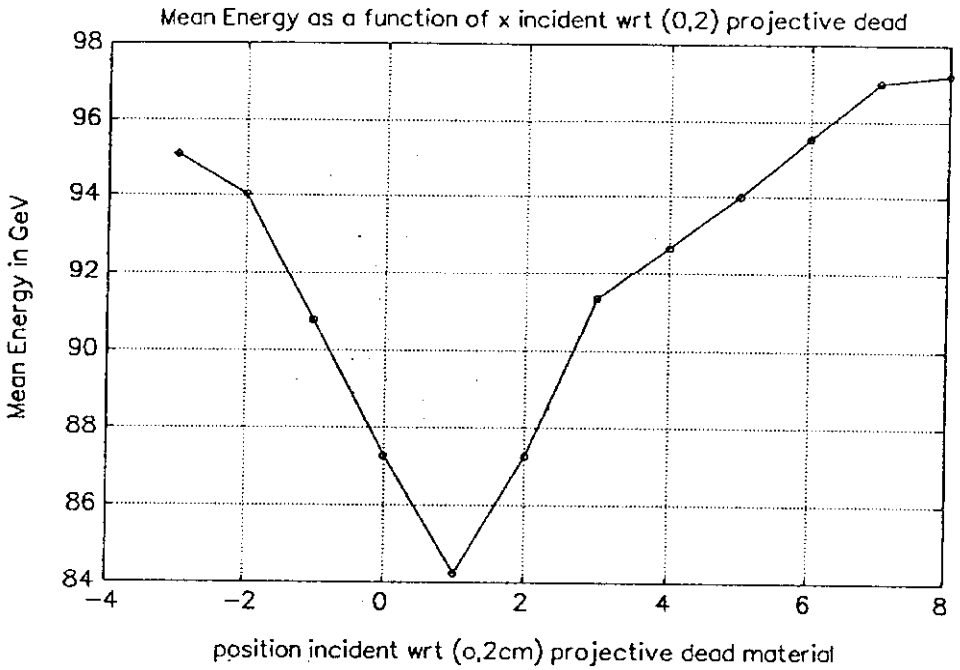

a)

Fig. 5.a.

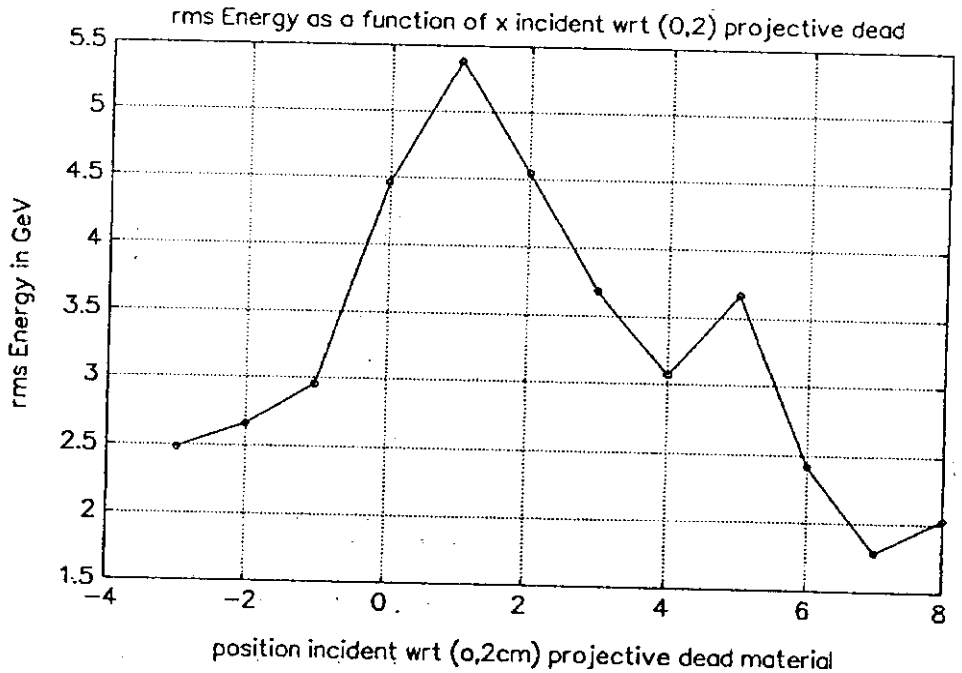

b)

Fig. 5.b.

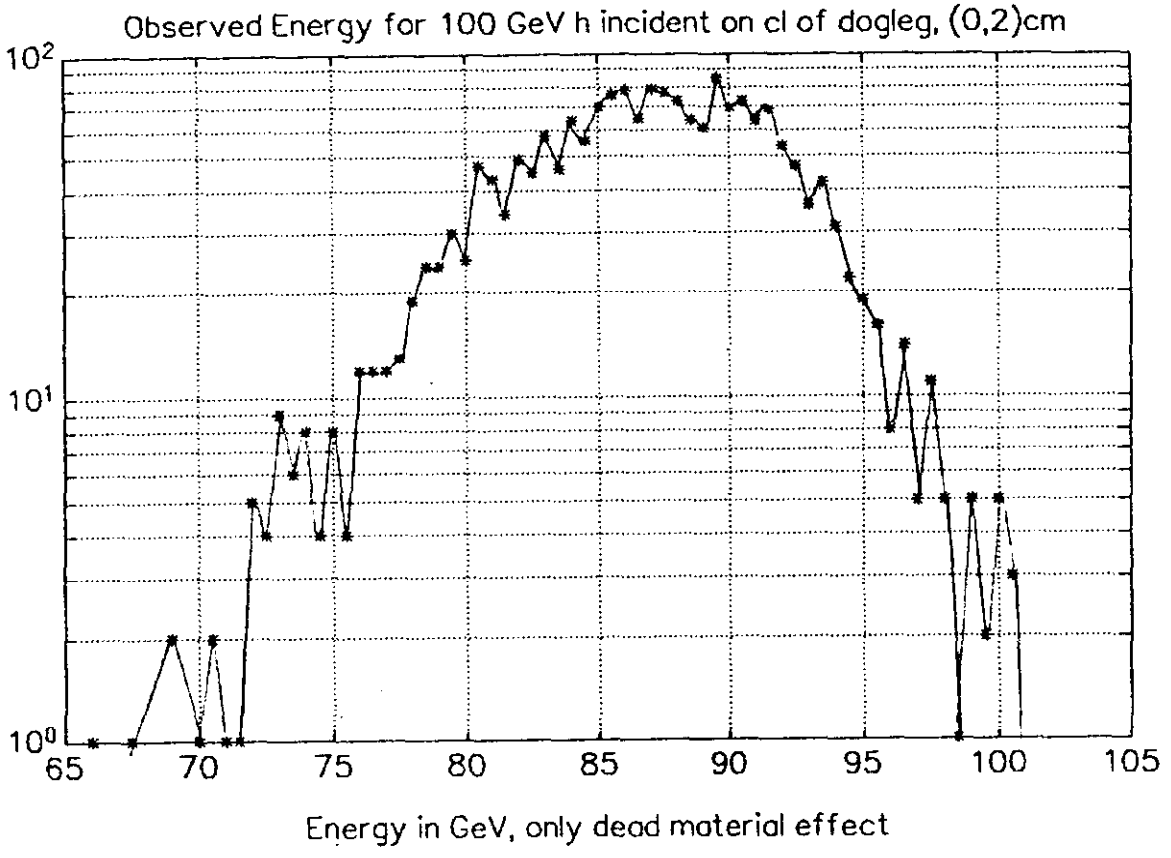
Observed Energy for 100 GeV h incident on cl of dogleg, (0,2)cm
10^2
10^1
10^0
65
70
75
80
85
90
95
100
105
Energy in GeV, only dead material effect

Fig. 6

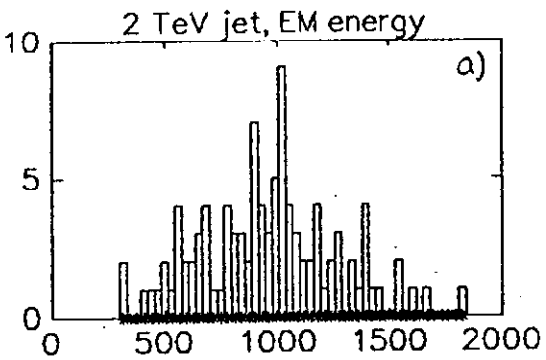

Fig. 7.a.

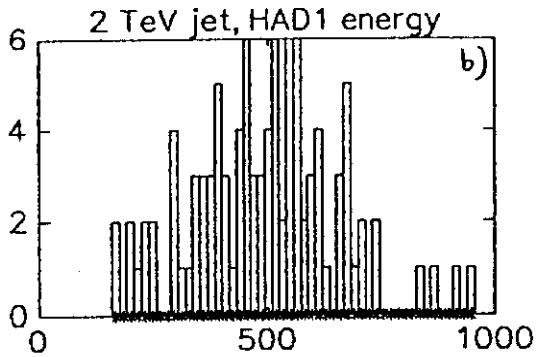

Fig. 7.b.

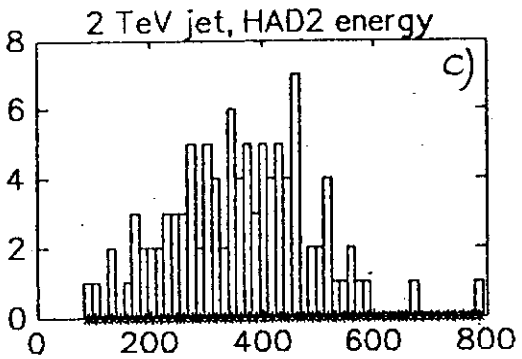

Fig. 7.c.

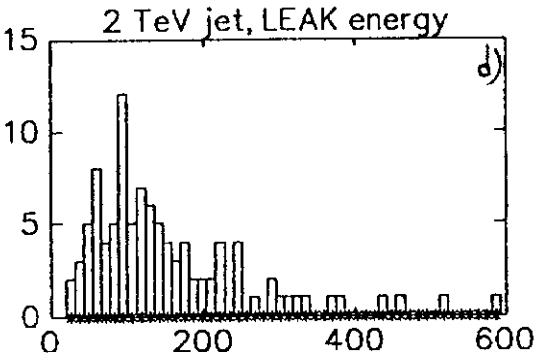

Fig. 7.d.

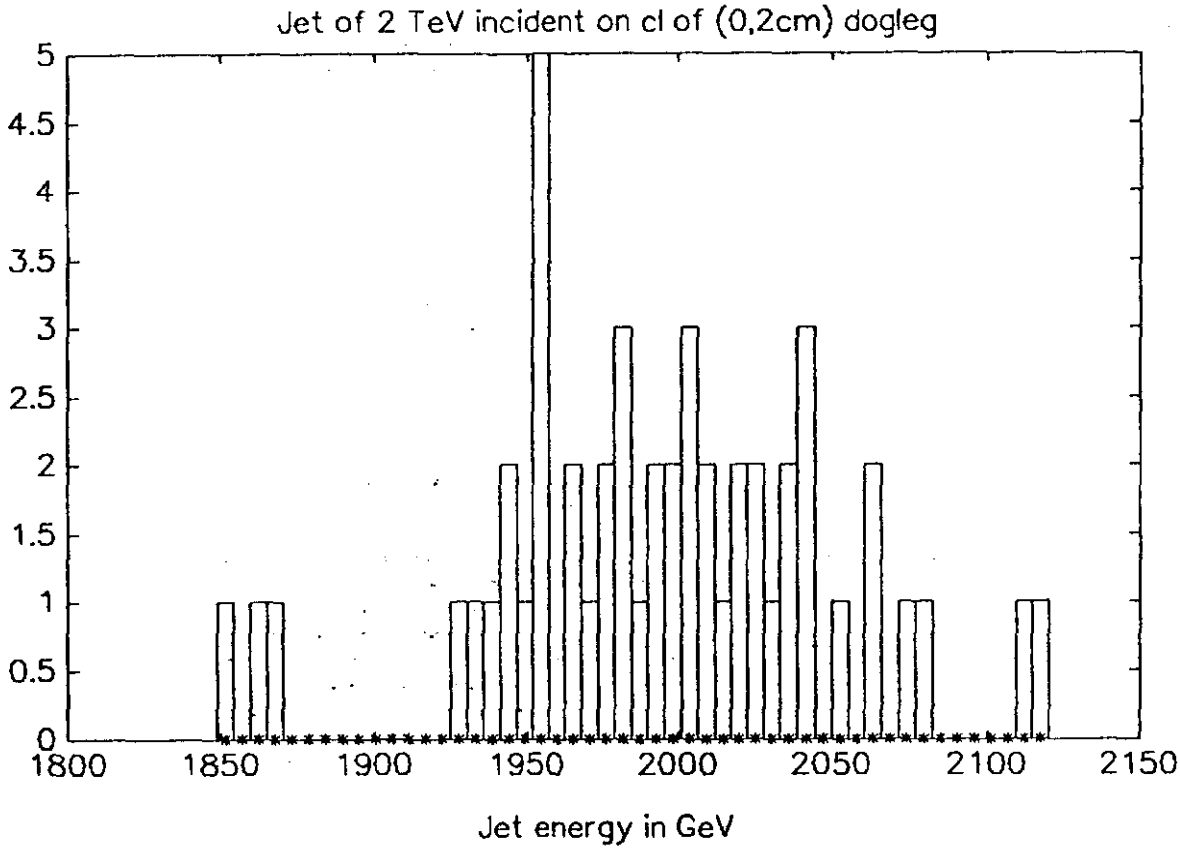
Jet of 2 TeV incident on cl of (0,2cm) dogleg
5
4.5
4
3.5
3
2.5
2
1.5
1
0.5
0
1800
1850
1900
1950
2000
2050
2100
2150
Jet energy in GeV

Fig. 8